Evidence for Interchange Ligand-Exchange Processes on Solvated Beryllium Cations

by **Ralph Puchta**[a])[b]), **Nico van Eikema Hommes**[a]), and **Rudi van Eldik***[b])

[a]) Computer Chemistry Center, University of Erlangen-Nürnberg, Nägelsbachstraße 25, D-91052 Erlangen
[b]) Institute for Inorganic Chemistry, University of Erlangen-Nürnberg, Egerlandstraße 1, D-91058 Erlangen
(e-mail: vaneldik@chemie.uni-erlangen.de)

Dedicated to Prof. *André Merbach* on the occasion of his 65th birthday

The ligand-exchange mechanism of solvated Be^{2+} cations has been studied by means of DFT calculations (RB3LYP/6-311 + G**). Ligand exchange around $[BeL_4]^{2+}$, where L = H_2O, NH_3, CO_2, formaldehyde (H_2CO), HCN, N_2, and CO, was found to follow an associative interchange (I_a) process in all cases. The size of the activation barrier is almost independent of the type of donor atom, and depends mainly on the hybridization undergone by the donor atom. This, in turn, suggests that steric effects play a major role in solvent- and ligand-exchange reactions in Be^{2+} systems.

Introduction. – Beryllium (Be), discovered in 1797 by *Vauquelin* and first isolated in 1828 by *Wöhler* and *Bussy*, plays a key role in a number of modern technologies: as a neutron moderator or reflector in nuclear reactors, in alloys with various metals in springs, electrical contacts, gyroscopes, satellites, and structural parts of the space shuttle, as metal foil in X-ray windows, or as oxide in ceramics [1–3]. In astronomy, the traceability of Be allows the investigation of the evolution of stars [4], as well as its use as a cosmic chronometer [5]. However, applications of and research on Be and its compounds are severely hampered by the very high toxicities of these materials [6]. As a consequence, accurate data are relatively scarce.

The reactivity of Be salts in solution is, in general, controlled by the lability of coordinated solvent molecules attached to Be^{2+} ions. This has been realized for a long time [7], and detailed studies on solvent-exchange reactions on Be^{2+} were performed by means of NMR techniques. Earlier mechanistic assignments were based on correlations between both stereochemistry and electron-donor ability of the solvent and its tendency to exchange with free solvent through a first-order and/or a second-order pathway in non-coordinating polar diluents [8]. Available temperature-dependent data from which mechanistic conclusions were drawn on the basis of activation enthalpy and entropy were, at that point, still subject to criticism and not clear-cut to interpret. For this reason, *Merbach* and co-workers [9] have applied high-pressure NMR techniques to study solvent-exchange reactions on Be^{2+}, from which activation-volume data of such processes could be obtained. The latter parameter has been illustrated in many studies to be a very reliable mechanistic indicator that enables an accurate description of the solvent-exchange mechanism [10]. It was found that second-order solvent-exchange reactions exhibit negative activation volumes typical for a limiting associative (A) or associative-interchange (I_a) mechanism, whereas first-order

exchange reactions exhibit large positive activation volumes typical for a limiting dissociative (D) exchange mechanism. The reported volumes of activation for the following series of exchanging solvents[1]) are -13.6 (H_2O), -2.5 (DMSO), -4.1 (TMP), -3.1 (DMF), $+10.5$ (TMU), and $+10.3$ (DMPU) $cm^3\ mol^{-1}$. The range of values was suggested to cover the whole range of limiting A- to D-mechanisms, respectively. The extreme values were argued to be close to those predicted by *Swaddle* for A-type ($-13\ cm^3\ mol^{-1}$) and D-type ($+13\ cm^3\ mol^{-1}$) H_2O exchange reactions in octahedral complexes [11]. This agreement may be fortuitous, since solvated Be^{2+} ions are *tetrahedrally* coordinated, and a comparison with the behavior of *octahedral* complexes may be a too rough approximation. Nevertheless, this does not affect the overall mechanistic interpretation, rather the detailed assignment of limiting *vs.* interchange mechanisms. We have, therefore, looked at theoretical ways to predict the nature of the transition state for such solvent-exchange reactions by means of density-functional-theory (DFT) calculations.

We have recently demonstrated the impressive advantage of modern high-level theoretical methods for the investigation of the mechanism of ligand-exchange reactions with Li^+ in water (H_2O) and ammonia (NH_3) [12]. This experience motivated us also to study the dynamics of the coordination chemistry of solvated Be^{2+} in various solvents by means of high-level DFT and *ab initio* computations. The main focus of this contribution will be on mechanistic details of ligand-exchange reactions in H_2O and NH_3, which will be compared with the behavior in various model solvents such as molecular nitrogen (N_2), hydrogen cyanide (HCN), carbon monoxide (CO), carbon dioxide (CO_2), and formaldehyde (H_2CO).

Experimental. – All structures were fully optimized at the B3LYP/6-311 + G** level [13], and characterized as minima or transition-state structures by computation of vibrational frequencies. For minima, all frequencies are positive ($N_{imag} = 0$); for transition-state structures, exactly one imaginary frequency is present ($N_{imag} = 1$). Single-point-energy calculations were performed at the B3LYP/6-311 + G** level, optimized structures were derived at MP2(full)/6-311 + G**//B3LYP/6-311 + G** level [14]; all electrons were included in the correlation treatment [15]. The influence of bulk solvent was probed with the IPCM formalism [16] with H_2O as solvent, and also employing the B3LYP/6-311 + G** structures, *i.e.*, B3LYP(IPCM)/6-311 + G**//B3LYP/6-311 + G**. Molecular volumes were computed as part of the IPCM calculations. Population analysis was performed with the Natural Bond Orbital analysis [17]. The Gaussian-98 suite of programs was used throughout [18].

Results und Discussion. – The calculated relative energies and molecular volumes of all species investigated are collected in the *Table*. Molecular structures, with relevant bond lengths, are shown in *Figs. 1–3*.

1. *Water Exchange*. Despite the smaller size and higher charge of Be^{2+} compared to Li^+ [12], the similarities between the aqua complexes are apparent. The first coordination shell consists of four H_2O molecules [6][9][19][20]. Both $[Be(H_2O)_4]^{2+}$ and $[Li(H_2O)_4]^+$ have tetrahedral structures in which the H_2O ligands have local C_{2v} symmetry, *i.e.*, the metal cation lies on the symmetry axis. This indicates that bonding is dominated by electrostatic ion–dipole interactions. Population analysis confirms that charge transfer from the O-atoms of H_2O to the cation is negligible. However, the effect

---

[1]) Abbreviations: DMSO, dimethylsulfoxide; TMP, trimethylphosphate; DMF, *N*,*N*-dimethylformamide; TMU, *N*,*N*,*N*,*N*-tetramethylurea; DMPU, '*N*,*N*'-dimethylpropyleneurea' (=3,4,5,6-tetrahydro-1,3-dimethylpyrimidin-2(1*H*)-one).

Table. *Calculated Relative Energies and Molecular-Volume Changes for Different Beryllium Complexes*

System[a])	Symmetry	N_{imag}	B3LYP [kcal/mol]	MP2(full) [kcal/mol]	IPCM [kcal/mol]	ΔV [Å^3]
$[Be(H_2O)_4]^{2+} + H_2O$	C_1	0, 0	+29.2	+29.3	+3.8	+2.7
$[Be(H_2O)_4(H_2O)]^{2+}$	C_2	0	0.0	0.0	0.0	0.0
$[Be(H_2O)_5]^{2+}$	C_2	1	+15.6	+12.6	+9.8	−4.5
$[Be(NH_3)_4]^{2+} + NH_3$	T_d	0, 0	+21.2	+21.8	+1.9	+7.3
$[Be(NH_3)_4(NH_3)]^{2+}$	C_1	0	0.0	0.0	0.0	0.0
$[Be(NH_3)_5]^{2+}$	C_{3h}	1	+18.8	+15.8	+17.3	+3.2
$[Be(H_2CO)_4]^{2+} + H_2CO$	C_1	0, 0	+19.8	+19.3	+3.9	+10.2
$[Be(H_2CO)_4(H_2CO)]^{2+}$	C_1	0	0.0	0.0	0.0	0.0
$[Be(H_2CO)_5]^{2+}$	C_1	1	+10.1	+3.3	+9.8	+4.6
$[Be(CO_2)_4]^{2+} + CO_2$	C_1	0, 0	+8.2	+11.2	+1.2	−2.5
$[Be(CO_2)_4(CO_2)]^{2+}$	C_1	0	0.0	0.0	0.0	0.0
$[Be(CO_2)_5]^{2+}$	C_1	1	+7.6	+5.9	−0.7	−7.7
$[Be(HCN)_4]^{2+} + HCN$	T_d	0, 0	+12.7	+16.3	−4.1	−2.6
$[Be(HCN)_4(HCN)]^{2+}$	C_{3v}	0	0.0	0.0	0.0	0.0
$[Be(HCN)_5]^{2+}$	D_{3h}	1	+4.3	+1.5	+3.9	−3.7
$[Be(N_2)_4]^{2+} + N_2$	T_d	0, 0	+5.5	+8.8	−3.1	+4.5
$[Be(N_2)_4(N_2)]^{2+}$	C_{3v}	0	0.0	0.0	0.0	0.0
$[Be(N_2)_5]^{2+}$	D_{3h}	1	+1.7	−0.3	+9.9	0.0
$[Be(OC)_4]^{2+} + CO$	T_d	0, 0	+4.7	+6.2	−15.7	−3.2
$[Be(OC)_4(OC)]^{2+}$	C_{3v}	0	0.0	0.0	0.0	0.0
$[Be(OC)_5]^{2+}$	D_{3h}	1	+2.6	+0.3	−0.7	−5.3
$[Be(CO)_4]^{2+} + CO$	T_d	0, 0	+7.5	+10.5	−11.5	+0.5
$[Be(CO)_4(CO)]^{2+}$	C_{3v}	0	0.0	0.0	0.0	0.0
$[Be(CO)_5]^{2+}$	D_{3h}	1	+4.7	+4.3	+3.7	−2.9

[a]) Complexes of the type $[Be(L)_5]^{2+}$, but not $[Be(L)_4(L)]^{2+}$, represent transtition-state structures ($N_{imag} = 1$). Note, OC and CO refer to O- *vs.* C-bound carbon monoxide.

of the double-positive charge of the metal is clearly seen. The $[Be(H_2O)_4]^{2+}$ complex is smaller than in $[Li(H_2O)_4]^+$, and the H_2O ligands are more-tightly bound in the former (computed Be–O *vs.* Li–O distances of 1.65 and 1.96 Å, resp.). Also, the complexation energy of the fourth H_2O molecule to Be^{2+}, 46.6 kcal/mol, is roughly three times higher than that computed for Li^+ (15.4 kcal/mol).

In both the Be^{2+} and Li^+ aqua complexes, further solvent molecules do not coordinate to the metal, but form a second solvation sphere instead, forming H-bonds to the four directly coordinated H_2O molecules of the first solvation sphere. The computed structures of the complexes $[Be(H_2O)_4(H_2O)]^{2+}$ (*Fig. 1*) and $[Li(H_2O)_4(H_2O)]^+$ are very similar: both lone pairs of the fifth H_2O molecule are involved in H-bonding to two coordinated H_2O molecules. Again, the higher charge on the central Be^{2+} cation leads to a stronger interaction: the fifth H_2O molecule is bound by 29.2 kcal/mol, relative to 12.2 kcal/mol in the corresponding Li^+ complex. However, these computed values are exaggerated: ion–molecule interaction energies are generally overestimated in the gas phase. Inclusion of the influence of bulk solvent by means of the IPCM model presents a more-appropriate picture: now, a binding energy for the fifth H_2O molecule of 3.8 kcal/mol is computed, relative to 4.6 kcal/mol for Li^+.

Merbach and co-workers have taken the activation volume of $-13.6\ cm^3\ mol^{-1}$ for H_2O exchange around Be^{2+} as a clear indication of an associative (A or I_a) exchange mode [9]. Based on the semi-empirical calculations developed by *Swaddle* [11], they favored an associative A-type mechanism, but a definitive conclusion was not possible. In addition, we previously found the exchange mechanism for H_2O around Li^+ to be a borderline case between A- and I_a-type; on the basis of the stronger binding within the Be^{II} complex, a true associative mechanism may even be more likely.

Our computations unequivocally reveal that this is not the case. The trigonal-bipyramidal penta-aqua complex $[Be(H_2O)_5]^{2+}$ is not an intermediate, but represents the transition state for H_2O exchange, energetically (B3LYP/6-311 + G**) lying 15.6 kcal/mol above the H-bonded penta-aqua complex $[Be(H_2O)_4(H_2O)]^{2+}$. The energy profile for the H_2O exchange process and the structures of the complexes are shown in *Fig. 1*.

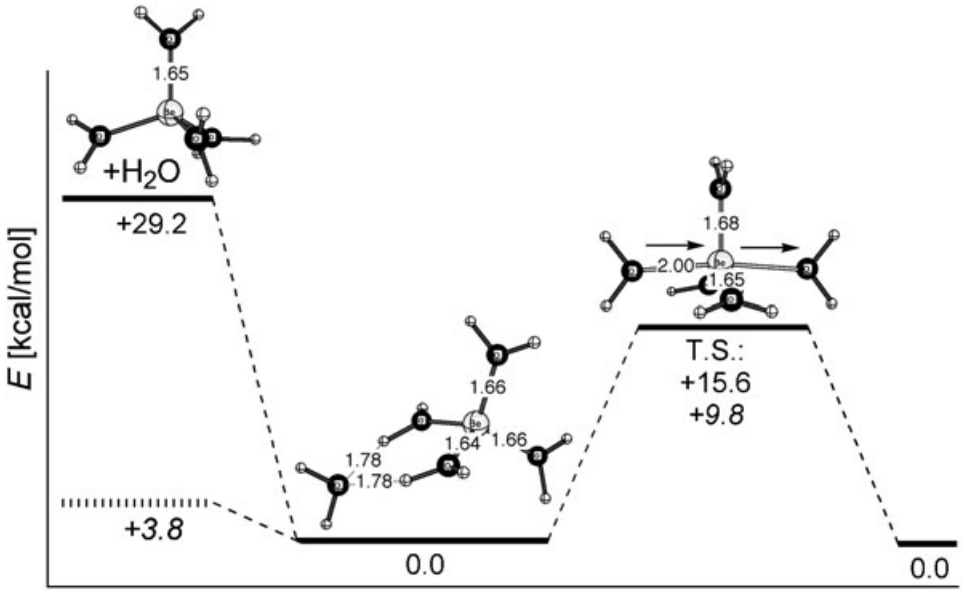

Fig. 1. *Energy profile for exchange of H_2O around Be^{2+}*. Distances in Å, energies in kcal/mol. Calculated at the B3LYP/6-311 + G** and B3LYP(IPCM)/6-311 + G** (values in italics) levels.

When the H-bonded H_2O molecule from the second solvation sphere approaches Be^{2+}, the previously H-bonded ligands assume equatorial positions. Ligand exchange then proceeds in a *trans* mode, similar to the well-known S_N2 mechanism. The ligand being expelled remains in the second solvation sphere, H-bonded to two metal-coordinated H_2O molecules.

The Be–ligand bonds in the transition-state structure deserve some comments. The three H_2O ligands not directly involved in the exchange process remain strongly bound to Be^{2+} during the reaction; the Be–O distances are essentially the same as in the precursor complex. The distances to the entering and leaving H_2O molecules are only

0.3 Å longer, indicating that the bonds to these ligands are strong, in line with an I_a-type mechanism.

To ascertain the reliability of the B3LYP hybrid density functional, we computed the MP2(full)/6-311 + G** energies for comparison, employing the structures obtained at the B3LYP/6-311 + G** level. The activation barrier at this level was found to be 12.6 kcal/mol. Note that activation barriers are generally somewhat underestimated by MP2 [14]. Inclusion of the influence of bulk solvent indeed leads to a moderate reduction of the activation energy. At the B3LYP(IPCM)/6-311 + G**//B3LYP/6-311 + G** level, we computed a barrier of 9.8 kcal/mol.

In the IPCM calculations, the molecule is contained inside a cavity within the polarizable continuum, the size of which is determined by a suitable computed isodensity surface. The size of this cavity corresponds to the molecular-volume parameter. This allows a simple, yet effective, evaluation of the molecular activation volume, which is not based on semi-empirical models. The computed molecular volumes are listed in the *Table*. The computed volume difference of -4.5 Å^3 between the precursor complex $[Be(H_2O)_4(H_2O)]^{2+}$ and the transition structure $[Be(H_2O)_5]^{2+}$ represents the activation volume of the reaction. This value can be compared with that computed for the corresponding H_2O exchange reaction around Li^+ (-6.1 Å^3), for which we concluded the operation of an I_a-type mechanism. In the present case, both the nature of $[Be(H_2O)_5]^{2+}$ and the activation volume clearly indicate an I_a-type mechanism. Thus, the compactness of the Be^{2+} center does not allow the coordination of five H_2O molecules with similar bond lengths that would be required to form a true five-coordinate intermediate, as was found in the case of Li^+. The bond lengthening observed for the entering and leaving H_2O molecules in the transition state (see *Fig. 1*) clearly points to the operation of an I_a-type process.

Note that the calculated molecular activation volumes cannot directly be compared to experimental values. The main reason for this is that the second solvation sphere is almost completely absent, only the incoming solvent molecule is taken into account. Explicit inclusion of the second solvation sphere is not feasible: apart from the significant increase in complexity of the structure optimization, a molecular-dynamics treatment would be required, which is not presently possible at the theoretical levels employed in this study. In addition, the IPCM calculations are based on structures that were optimized without the solvent continuum, but the influence of this approximation is expected to be minor.

2. *Ammonia Exchange*. Whereas the behavior of Be^{2+} in H_2O is of practical importance, the mechanism of NH_3 exchange around Be^{2+} may, at first, appear to be of academic interest only. Nevertheless, as we have demonstrated in the case of exchange around Li^+ [12], a comparison of ligands with different donor atoms is instructive. The differences in size between H_2O and NH_3, as well as in bond strength between Li–O and Li–N bonds, cause NH_3 exchange around Li^+ to proceed *via* an I_a-type mechanism. In the case of the solvated Be^{2+} dication, the Be–N bond is computed to be somewhat stronger than the Be–O bond: the complexation energies for the fourth ligand molecule are 46.6 and 48.1 kcal/mol for H_2O and NH_3, respectively.

As in the case of the aqua complex, four NH_3 molecules can coordinate directly to Be^{2+}. The resulting $[Be(NH_3)_4]^{2+}$ complex has a tetrahedral geometry, the Be–N bond length being 1.77 Å. Additional NH_3 molecules form a second solvation sphere. The

structure of $[Be(NH_3)_4(NH_3)]^{2+}$, however, does not show a bifurcated H-bond to two coordinating NH_3 molecules, as in the case of $[Li(NH_3)_4(NH_3)]^+$. The fifth NH_3 molecule forms a single H-bond to one coordinating NH_3. The computed interaction energy of 21.2 kcal/mol is significantly higher than that computed at the same theoretical level for $(NH_3)_2$ (1.8 kcal/mol). As in the case of the aqua complex, the large electrostatic contribution leads to an exaggerated binding energy, as confirmed by IPCM calculations. Modeling the influence of bulk solvent results in a binding energy for the fifth NH_3 molecule of only 1.9 kcal/mol.

The energy profile for the solvent-exchange reaction and the structures involved are shown in *Fig. 2*. Exchange of NH_3 around Be^{2+} also proceeds through an S_N2-like, trigonal-bipyramidal transition structure $[Be(NH_3)_5]^{2+}$, with an activation barrier of 18.8 kcal/mol. Thus, the rate of the exchange reaction will be similar to or somewhat slower than in the case of H_2O. The Be–N distances for the incoming and leaving NH_3 molecule, 2.29 Å, are more than 0.5 Å longer than the other Be–N bonds (these vary very little throughout the process). This elongation, however, reflects the higher steric demand of NH_3 compared to H_2O (for which an elongation of 0.28 Å was computed [12]), rather than a change in mechanism.

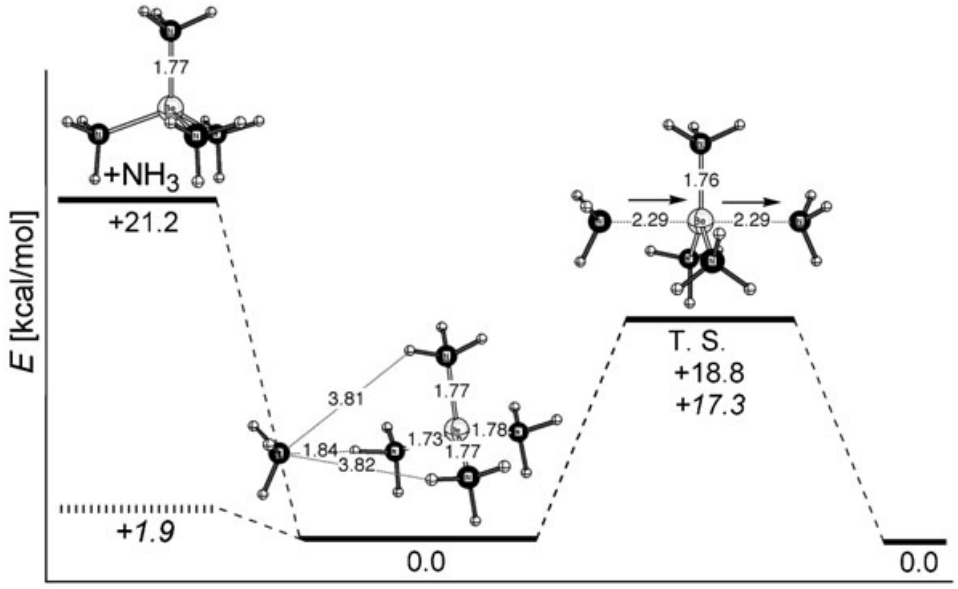

Fig. 2. *Energy profile for exchange of NH_3 around Be^{2+}*. Distances in Å, energies in kcal/mol. Calculated at the B3LYP/6-311 + G** and B3LYP(IPCM)/6-311 + G** (values in italics) levels.

As expected (see above), at the MP2(full)/6-311 + G** level, a somewhat lower activation barrier of 15.7 kcal/mol was computed for NH_3 exchange. On the other hand, the influence of bulk solvent on the activation barrier appears to be small: at the B3LYP(IPCM)/6-311 + G** level, we calculated an activation barrier of 17.3 kcal/mol.

Compared to the complex $[Be(NH_3)_4]^{2+}$ plus a free NH_3 molecule, the molecular volume of the precursor $[Be(NH_3)_4(NH_3)]^{2+}$ is 7.3 $Å^3$ smaller than that of the reactants.

The transition structure is 3.1 Å^3 larger than in the case of $[Be(NH_3)_4(NH_3)]^{2+}$. The same increase in molecular volume was calculated for the NH_3 exchange around Li^+, for which an I_a-type mechanism is operative [12]. In the present case of NH_3 exchange around Be^{2+}, the same conclusion can, thus, be drawn.

3. *Other Ligands and Influence of Hybridization.* With the exception of H_2O, all solvents investigated by *Merbach* and co-workers [9], *i.e.*, DMSO, TMP, DMF, TMU, and DMPU[1]), coordinate to Be^{2+} *via* a donor O-atom that is double bonded to a heteroatom. This suggests that coordinative bonding will be similar for all solvents, and differences in the exchange mechanism will largely be due to steric influences. In the present study, we decided to model these solvents with the smallest carbonyl compound: formaldehyde (H_2CO). Apart from drastically reducing the size of the complexes, this has the advantage that conformational artifacts due to flexible substituents are avoided. Furthermore, the recent increase in interest in alternative reaction media, like supercritical CO_2 [21] or ionic liquids [22][23], as well as their use in industrial applications [24][25], prompted us to include a number of small, both polar and non-polar molecules as ligands (L) in this investigation: CO_2, HCN (a H_2O-like, ionizing solvent [26] and a computational model for MeCN), N_2, and CO. For carbon monoxide, both possible coordination modes to the C- and O-atoms were investigated. This series of ligands, together with H_2O and NH_3 discussed above, allows us to compare the coordinating properties of O-, N-, and C-based donor atoms, as well as to study the influence of the chemical environment of the coordinating atom in terms of the differences between sp^3, sp^2, and sp hybridization (see below).

The calculated structures of the precursor complexes $[Be(L)_4L]^{2+}$ and the penta-coordinate structures $[Be(L)_5]^{2+}$ are shown in *Fig. 3*. In all cases, the calculation of vibrational frequencies reveals that $[Be(L)_5]^{2+}$ is a transition-state structure ($N_{imag} = 1$), *i.e.*, our calculations predict that ligand exchange proceeds *via* an interchange-type (I_a) mechanism. All precursor complexes represent energy minima ($N_{imag} = 0$).

Since no H-bonds are possible between the incoming ligand L and the metal-bound ligands, the fifth ligand is bound to $[Be(L)_4]^{2+}$ by electrostatic forces only. The high positive charge on the Be^{2+} dication polarizes the incoming ligand, which leads to an induced dipole moment. Bonding is caused by the attractive interaction between the metal ion and the dipole of the ligand, *i.e.*, the sum of the induced dipole and the dipole moment of the ligand itself. Compared to H_2O and NH_3, the interaction energy is much weaker for the other studied ligands. As expected, inclusion of the influence of bulk solvent strongly reduces the interaction energies. In the case of CO, the B3LYP(IPCM) calculations even indicate that the fifth CO molecule will not bind to the tetra-coordinate complex. The structures of the precursor complexes $[Be(L)_4L]^{2+}$ (where $L = N_2$, HCN, and CO or OC)[2]) already show the characteristics of the corresponding transition-state structures, *viz.*, the Be–L distance for the ligand *trans* to the incoming ligand is lengthened by 0.02–0.03 Å. No lengthening is apparent for $L = CO_2$, but the picture is blurred here by the lack of symmetry in the complex.

With the exception of $L = CO_2$, the transition structures are highly symmetrical. The Be–L bonds to the incoming and the leaving ligand are between 0.23 and 0.40 Å longer than the other Be–ligand bonds. Such elongations are typical for an I_a-type

---

[2]) Note, CO and OC represent O- *vs.* C-bound carbon monoxide ligands.

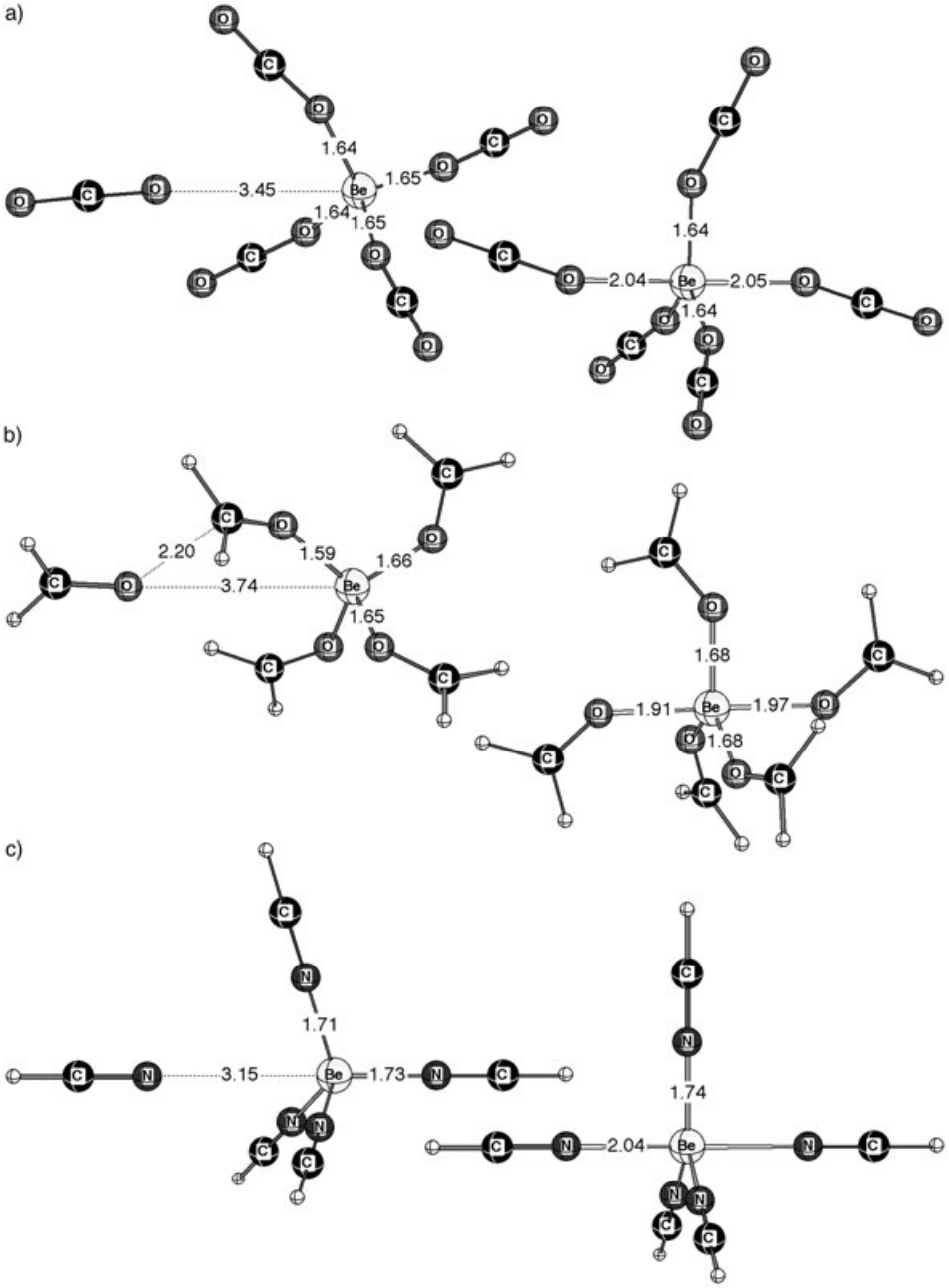

Fig. 3. *Structures of precursor complexes and ligand-exchange transition states for* a) *carbon dioxide* (CO_2), b) *formaldehyde* (H_2CO), c) *hydrogen cyanide* (HCN), d) *molecular nitrogen* (N_2), *and* e) *carbon monoxide* (OC *vs.* CO)[2])

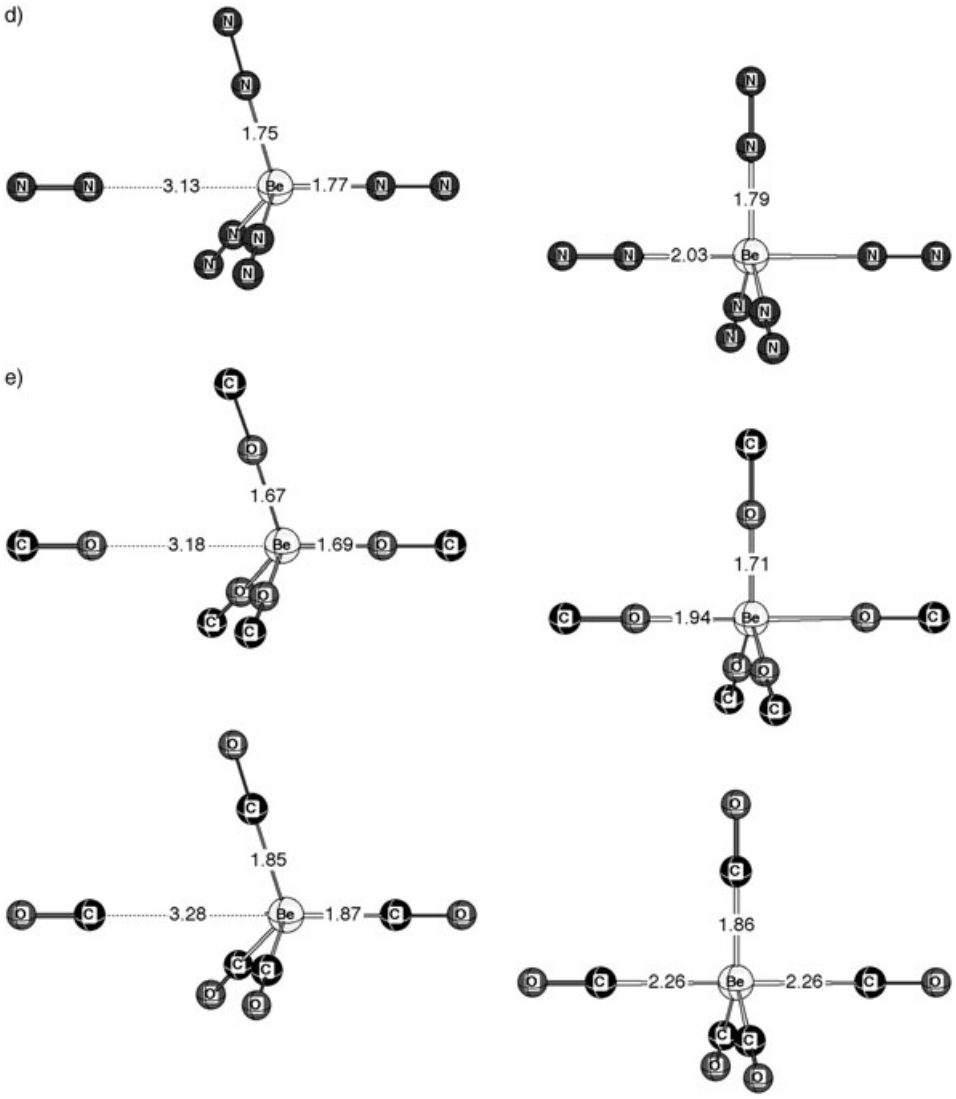

Fig. 3 (cont.)

mechanism. The molecular volumes support this: except for $L = N_2$, the transition-state structures $[Be(L)_5]^{2+}$ are more compact than the precursor complexes $[Be(L)_4L]^{2+}$. The activation barriers are relatively low, indicating fast exchange.

The case of formaldehyde (H_2CO) is exceptional: the precursor complex is almost 20 kcal/mol more stable than $[Be(H_2CO)_4]^{2+}$ plus one free H_2CO molecule, despite the very long Be–O distance of 3.74 Å. However, the fifth ligand molecule is bound indirectly: its O-atom does not interact with Be^{2+}, but, instead, with the carbonyl C-atom of one of the coordinated H_2CO molecules. The C=O bond of this molecule is

polarized by the high positive charge of the Be^{2+} dication; this increases the positive charge on the carbonyl C-atom, which, in turn, leads to an attraction of the O-atom of the incoming H_2CO molecule. As a consequence, the computed O–C distance is only 2.20 Å, while the O–Be bond is shortened by 0.06 Å. Unfortunately, it is difficult to estimate the energetic preference over a hypothetical structure without the close C–O contact, since this would be a partially optimized structure. Thus, the activation barrier is biased and likely to be computed too high. Note also that the structure of the complex was optimized without including the influence of bulk solvent.

The unusual structure of the precursor complex, however, has no influence on the course of the exchange reaction, which proceeds *via* a similar transition structure as found for the other ligands discussed here. The 'active' Be–O bonds are elongated by 0.3 Å. The difference in bond length between the incoming and leaving H_2CO ligands results from the asymmetry caused by the nonlinear coordination of the carbonyl O-atom to Be^{2+}. The molecular volume increases in the transition structure, but this is likely to be due to the uncommon bonding situation in the precursor complex. In this case, an I_a-type mechanism is also operating.

Which factors determine the height of the activation barrier for exchange around Be^{2+}? There appears to be little, if any, influence of the coordinating donor atom. In the case of O-based donor ligands, the computed barriers vary between 2.6 and 15.6 kcal/mol, while a range from 1.7–18.8 kcal/mol is obtained for N-atoms.. For carbon (exchange of C-bound CO), a barrier of 4.7 kcal/mol is calculated.

It is instructive to compare the computed activation barriers for all ligands considered in this study. Relatively high activation barriers are calculated for the exchange of H_2O and NH_3 on Be^{2+}, whereas very low barriers are computed for HCN, CO, and N_2; CO_2 and H_2CO lie in between. This suggests that the activation barrier is determined by the nature of the lone pair, *i.e.*, the hybridization of the coordinating atom. The natural bond orbital analysis provides the hybridization of individual hybrid orbitals and lone pairs by means of the natural localized molecular orbital (NLMO) analysis [17]. The result of this approach is shown in *Fig. 4*, in which the activation barriers for ligand exchange are plotted against the p contribution in the NLMO hybridization of the lone pairs of the coordinating atoms.

Formally, the lone pairs on N_2, HCN, and CO are sp-hybridized. The NLMO hybridizations show even lower p contributions. Hence, these lone pairs have low directionality, electron density remains close to the coordinating atom, and interaction between the lone pair and Be^{2+} is comparatively weak. The Be–ligand bonds are easily disrupted, and ligand exchange, consequently, can proceed with a low activation barrier. A high degree of p character, in contrast, means that the lone pair is directed toward Be^{2+}, with electron density close to the metal center, and, thus, well suited for coordination. Hence, a strong interaction and a high ligand-exchange activation barrier result, which is what we compute for H_2O and NH_3. Ligands with double-bonded O-atoms assume an intermediate position.

Conclusions. – For all ligand-exchange reactions around Be^{2+} studied with small, slim ligands, we found an associative interchange (I_a-type) mechanism characterized by a clear activation barrier. Interestingly, the size of the activation barrier is almost independent of the type of donor atom; it depends mainly on the hybridization

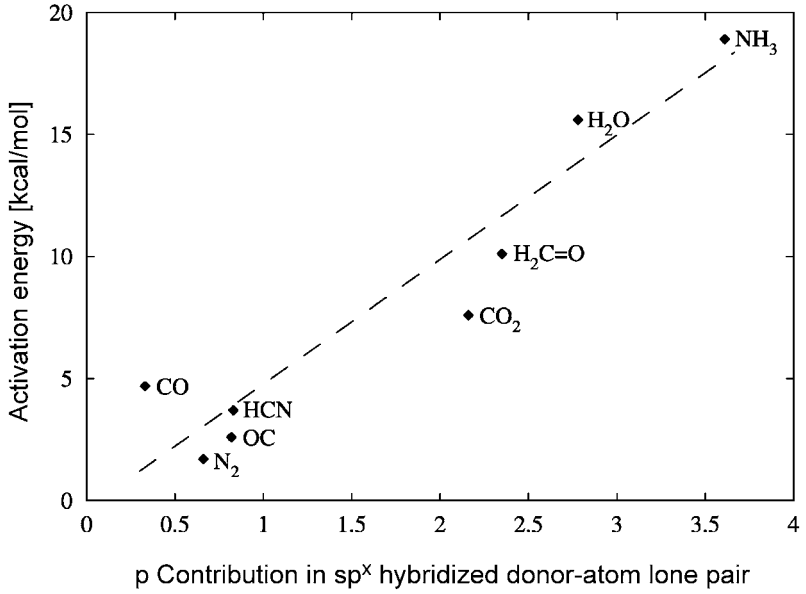

Fig. 4. *Relationship between computed activation energy* (B3LYP/6-311 + G**) *and p contribution in the NLMO hybridization of lone pairs on coordinating atoms*

undergone by the ligand donor atom. This, in turn, means that steric effects will play a major role in solvent-exchange reactions in Be^{2+} systems. The changeover in solvent-exchange mechanism from associative to dissociative observed by *Merbach* and co-workers [9] on going from less to more sterically crowded solvent molecules clearly demonstrates that solvent crowding determines the nature of the transition state for the exchange process. In this way, a three-coordinate transition state is favored in the dissociative, and a five-coordinate transition state in the associative exchange mechanism, respectively.

Financial support from the *European Commission* (contracts no. HPRN-CT-2000-19 and MRTN-CT-2003-503864) and from the *Deutsche Forschungsgemeinschaft* (SFB 583: 'Redox-Active Metal Complexes') is gratefully acknowledged. Prof. *Tim Clark* is kindly acknowledged for his support of this work. We thank the *Regionales Rechenzentrum Erlangen* (*RRZE*) for generous allotment of computer time.

REFERENCES

[1] G. Petzkow, H. Zorn, *Chem.-Ztg.* **1974**, *98*, 236.
[2] T. Takagi, K. Matsubara, *J. Appl. Phys.* **1980**, *51*, 5419.
[3] A. Seidel, 'Gemelins Handbook of Inorganic Chemistry – Beryllium Supplement A1', Springer, Berlin, 1986, p. 300.
[4] F. Primas, M. Asplund, P. E. Nissen, V. Hill, *Astron. Astrophys.* **2000**, *364*, L42 – 46.
[5] L. Pasquini, P. Bonifacio, S. Randich, D. Galli, R. G. Gratton, *Astron. Astrophys.* **2004**, *426*, 651.
[6] O. Kumberger, H. Schmidbaur, *Chemie unserer Zeit* **1993**, *27*, 310; L. S. Newman, *Chem. Eng. News* **2003**, *81*, 38.
[7] S. F. Lincoln, M. N. Tkaczuk, *Ber. Bunsenges. Phys. Chem.* **1981**, *85*, 433.
[8] S. F. Lincoln, M. N. Tkaczuk, *Ber. Bunsenges. Phys. Chem.* **1982**, *86*, 221.

[9] P.-A. Pittet, G. Elbaze, L. Helm, A. E. Merbach, *Inorg. Chem.* **1990**, *29*, 1936.
[10] F. A. Dunand, L. Helm, A. E. Merbach, *Adv. Inorg. Chem* **2003**, *54*, 1; R. van Eldik, C. D. Hubbard, in 'Chemistry at Extreme Conditions', Ed. M. Riad Manaa, Elsevier, Amsterdam, 2005, Chapt. 4.
[11] T. W. Swaddle, *Inorg. Chem.* **1983**, *22*, 2663.
[12] R. Puchta, M. Galle, N. van Eikema Hommes, E. Pasgreta, R. van Eldik, *Inorg. Chem.*, in press.
[13] P. J. Stevens, F. J. Devlin, C. F. Chablowski, M. J. Frisch, *J. Phys. Chem.* **1994**, *98*, 11623; A. D. Becke, *J. Chem. Phys.* **1993**, *98*, 5648; C. Lee, W. Yang, R. G. Parr, *Phys. Rev. B* **1988**, *37*, 785; W. Koch, M. C. Holthausen, 'A Chemist's Guide to Density Functional Theory', 2nd edn., Wiley-VCH, Weinheim, 2001, Chapt. 13.
[14] W. J. Hehre, L. Radom, P. v. R. Schleyer, J. A. Pople, 'Ab Initio Molecular Orbital Theory', Wiley, New York, 1986.
[15] H. Hofmann, E. Hänsele and T. Clark, *J. Comput. Chem*. **1990**, *11*, 1147.
[16] J. B. Foresman, T. A. Keith, K. B. Wiberg, J. Snoonian M. J. Frisch, *J. Phys. Chem.* **1996**, *100*, 16098.
[17] A. E. Reed, L. A. Curtiss, F. Weinhold, *Chem. Rev.* **1988**, *88*, 899 and refs. cit. therein.
[18] M. J. Frisch, G. W. Trucks, H. B. Schlegel, G. E. Scuseria, M. A. Robb, J. R. Cheeseman, V. G. Zakrzewski, J. A. Montgomery Jr., R. E. Stratmann, J. C. Burant, S. Dapprich, J. M. Millam, A. D. Daniels, K. N. Kudin, M. C. Strain, O. Farkas, J. Tomasi, V. Barone, M. Cossi, R. Cammi, B. Mennucci, C. Pomelli, C. Adamo, S. Clifford, J. Ochterski, G. A. Petersson, P. Y. Ayala, Q. Cui, K. Morokuma, N. Rega, P. Salvador, J. J. Dannenberg, D. K. Malick, A. D. Rabuck, K. Raghavachari, J. B. Foresman, J. Cioslowski, J. V. Ortiz, A. G. Baboul, B. B. Stefanov, G. Liu, A. Liashenko, P. Piskorz, I. Komaromi, R. Gomperts, R. L. Martin, D. J. Fox, T. Keith, M. A. Al-Laham, C. Y. Peng, A. Nanayakkara, M. Challacombe, P. M. W. Gill, B. Johnson, W. Chen, M. W. Wong, J. L. Andres, C. Gonzalez, M. Head-Gordon, E. S. Replogle, J. A. Pople, Gaussian 98, Revision A11.3, Gaussian, Inc., Pittsburgh, PA, 1998.
[19] D. N. Skilleleter, *Chem. Ber.* **1990**, *26*, 26.
[20] H. Schmidbaur, *Coord. Chem. Rev.* **2001**, *215*, 223.
[21] S. L. Wells, J. M. DeSimone, *Angew. Chem., Int. Ed.* **2001**, *29*, 535.
[22] P. Wasserscheid, T. Welton, Eds., 'Ionic Liquids in Synthesis', Wiley-VCH, Weinheim, 2003.
[23] C. F. Weber, R. Puchta, R. van Eldik, *Inorg. Chem.*, in preparation.
[24] K. Zosel, *Angew. Chem., Int. Ed.* **1978**, *17*, 702; M. D. A. Saldaña, R. S. Mohamed, P. Mazzafera, *Braz. J. Chem. Eng.* **2000**, *17*, 251.
[25] M. Volland, V. Seitz, M. Maase, M. Flores, R. Papp, K. Massonne, V. Stegmann, K. Halbritter, R. Noe, M. Bartsch, W. Siegel, M. Becker, O. Huttenloch, to *BASF AG*, WO 2003/062251,200.
[26] J. Jander, Ch. Lafrenz, 'Wasserähnliche Lösungsmittel', VCH, Weinheim, 1968.

Received November 23, 2004